Feasibility study of helical tomotherapy for total body or total marrow irradiation[a)]

Susanta K. Hui[b)]
Department of Therapeutic Radiology, University of Minnesota, Minneapolis, 420 Delaware Street SE, Minneapolis, Minnesota 55455
and Departments of Human Oncology, University of Wisconsin—Madison, 600 Highland Avenue, Madison, Wisconsin 53792

Jeff Kapatoes
Tomotherapy Incorporated, 1240 Deming Way, Madison, Wisconsin 53717

Jack Fowler
Departments of Human Oncology, University of Wisconsin—Madison, 600 Highland Avenue, Madison, Wisconsin 53792

Douglas Henderson and Gustavo Olivera
Tomotherapy Incorporated, 1240 Deming Way, Madison, Wisconsin 53717

Rafael R. Manon
Departments of Human Oncology, University of Wisconsin—Madison, 600 Highland Avenue, Madison, Wisconsin 53792

Bruce Gerbi
Department of Therapeutic Radiology, University of Minnesota, Minneapolis, 420 Delaware Street SE, Minneapolis, Minnesota 55455

T. R. Mackie
Tomotherapy Incorporated, 1240 Deming Way, Madison, Wisconsin 53717 and Departments of Human Oncology, University of Wisconsin—Madison, 600 Highland Avenue, Madison, Wisconsin 53792

James S. Welsh
Departments of Human Oncology, University of Wisconsin—Madison, 600 Highland Avenue, Madison, Wisconsin 53792

(Received 26 April 2005; revised 1 August 2005; accepted for publication 3 August 2005; published 29 September 2005)

Total body radiation (TBI) has been used for many years as a preconditioning agent before bone marrow transplantation. Many side effects still plague its use. We investigated the planning and delivery of total body irradiation (TBI) and selective total marrow irradiation (TMI) and a reduced radiation dose to sensitive structures using image-guided helical tomotherapy. To assess the feasibility of using helical tomotherapy, (**A**) we studied variations in pitch, field width, and modulation factor on total body and total marrow helical tomotherapy treatments. We varied these parameters to provide a uniform dose along with a treatment times similar to conventional TBI (15–30 min). (**B**) We also investigated limited (head, chest, and pelvis) megavoltage CT (MVCT) scanning for the dimensional pretreatment setup verification rather than total body MVCT scanning to shorten the overall treatment time per treatment fraction. (**C**) We placed thermoluminescent detectors (TLDs) inside a Rando phantom to measure the dose at seven anatomical sites, including the lungs. A simulated TBI treatment showed homogeneous dose coverage (±10%) to the whole body. Doses to the sensitive organs were reduced by 35%–70% of the target dose. TLD measurements on Rando showed an accurate dose delivery (±7%) to the target and critical organs. In the TMI study, the dose was delivered conformally to the bone marrow only. The TBI and TMI treatment delivery time was reduced (by 50%) by increasing the field width from 2.5 to 5.0 cm in the inferior–superior direction. A limited MVCT reduced the target localization time 60% compared to whole body MVCT. MVCT image-guided helical tomotherapy offers a novel method to deliver a precise, homogeneous radiation dose to the whole body target while reducing the dose significantly to all critical organs. A judicious selection of pitch, modulation factor, and field size is required to produce a homogeneous dose distribution along with an acceptable treatment time. In addition, conformal radiation to the bone marrow appears feasible in an external radiation treatment using image-guided helical tomotherapy. [DOI: 10.1118/1.2044428]

Key words: total body irradiation (TBI), total marrow irradiation (TMI), tomotherapy, MVCT, limited MVCT

I. INTRODUCTION

Total body irradiation (TBI) in conjunction with chemotherapy is a widely used preconditioning regimen for a bone marrow transplant (BMT). It provides immunosuppression, which helps in accepting the donor transplant. TBI also contributes to the eradication of radiosensitive malignant cells, thereby helping the donor marrow cells to repopulate the bone marrow. Clinical data and understanding of the radiobiology of TBI have led to more effective TBI dose-fractionation schedules and techniques. With increasing survival rates,[1–3] evaluation of side effects, and quality of life are important areas of investigation. TBI is primarily limited by the toxicity to critical organs, especially lung, eyes, heart, liver, and kidneys.[4–25] With the introduction of helical tomotherapy, a new potential exists to conform the dose to very specific areas of the body. This capability would allow marrow-only irradiation or irradiation of the total body while reducing the radiation dose to the lungs, heart, eyes, kidneys, and other internal organs. Here we present a brief survey of radiation effects on critical organs for TBI treatment in order to determine dose constraints, the development required for treatment planning optimization, dose delivery, and verifications. We then describe our application of this information for helical tomotherapy-based treatment planning for total marrow irradiation and selective organ-sparing total body irradiation.

II. DOSE LIMITS FOR ORGANS AT RISK

The primary dose-limiting factor in TBI regimens is lung toxicity.[6–10] Aldo *et al.*[6] observed that pulmonary complications increased from 3.8% to 19.2% when the dose of lung irradiation was above 9.4 Gy. In children, partial lung shielding has resulted in decreased lung toxicity.[11] The preservation of a respiratory function is especially important because of the high cure rates and long life expectancy of bone marrow transplant recipients, particularly children. Cataract formation[12–14] is the frequent late onset complication of TBI. A cataract incidence was observed when the radiation dose to lenses was above 8 Gy for a single fraction TBI treatment.[13] However, eye shielding reduced the cataract incidence to 31% compared to 90% without shielding.[13,14] In general, eye shielding has not been employed in most centers due to the reduced dose to the orbit, which can be a site of recurrent disease.[13] Long-term renal toxicity is another occasional adverse effect of conventional TBI.[15–19] Lawton *et al.*[19] found that the radiation threshold for renal damage was 10 Gy, beyond which renal shielding should be seriously considered. In their study, the BMT nephropathy incidence was 26% for unshielded patients (renal dose 14 Gy) compared to 6% in the shielded patients (renal dose reduced to 11.9 Gy). Although veno-oclusive disease (VOD) of the liver was often caused by chemotherapy,[20,21] Girinsky *et al.*[22] showed the possible occurrence of VOD above a 10 Gy radiation dose for a single fraction. However, it was negligible when fractionated TBIs of 14.85 Gy were used. Cardiac complications may result from chemotherapy or irradiation.[23,24] Blum *et al.*[25] reported a significant risk of cardiac toxicity (15% cardiac mortality), when poor-risk AL amyloidosis patients were treated with single fraction TBI of 5.5 Gy and chemotherapy for autologous transplantation. However, the threshold for a radiation effect has not yet been established.

III. POTENTIAL SOLUTIONS

Numerous techniques have been developed to reduce the toxicity of TBI.[26–30] Fractionation approaches were adopted to reduce the toxicity to critical organs (most of which have low α/β and to help in the cellular repair process of healthy tissues).[31] Despite low doses, toxicities remain quite high and shielding has been advocated to reduce the adverse effects of radiation. It can be a daunting task to create external shielding that accurately reflects the geometry of the organ of concern, and to accurately position the shielding every day. We have previously demonstrated[32] that sometimes lung shielding did not meet expectations, and advocated CT-based treatment and dose statistics. In addition, compensators and shielding can reduce the dose to the sites of recurrence.[33,34]

We present here a novel approach for TBI treatment with helical tomotherapy. Helical tomotherapy is a relatively new treatment option[35–37] that provides MVCT-based image guidance and intensity-modulated radiotherapy using a fan beam of radiation. Performing a MVCT before the treatment improves the accuracy of the treatment delivery. Operating the detector during treatment introduces the possibility of dose verification.[38] The tomotherapy machine consists of a 6 MV linear accelerator mounted on a ring gantry that rotates isocentrically around the patient as the patient is translated through the bore, yielding a helical path of radiation delivery. The maximum field size is 40 cm wide in the transverse direction. A binary multileaf collimator containing 64 leaves provides intensity modulation capabilities. For the inferior–superior direction, a movable set of tungsten jaws collimates the width of the fan beam slice width from fully closed to 5 cm wide.

We have investigated the conformal avoidance of critical organs in TBI using image-guided helical tomotherapy. We used this image-guided IMRT approach without external compensation to plan a homogeneous dose throughout the whole body while maintaining lower doses to sensitive structures. A plan was also generated for conformal irradiation of the marrow (TMI). In the planning process for both approaches, we conducted various studies to understand the effects of the available planning/machine parameters on target dose homogeneity as well as on the conformal avoidance of critical organs. The verification of dose delivery was

achieved experimentally using TLDs placed in a Rando phantom. Setup verification using MVCT, related error, and consequent dose effects were also studied.

IV. METHODS

We investigated the following aspects: (a) TBI planning and optimization, (b) TMI planning and optimization, (c) dose delivery verification, and (d) MVCT imaging for target localization. For the TBI and TMI planning study, a partial (3/4) whole body CT image was obtained from the PET/CT database. The resulting images were transferred to the TomoTherapy HiArt Planning Station (Tomotherapy, Inc., Madison, WI). The planning treatment volumes (PTVs) and critical organs were outlined for each slice. PTV1 represents the whole body, excluding organs at risk (OARs). Among others, OARs considered here were the lungs, eyes, heart, liver, and kidneys. PTV2 represents the bone targets that are active bone marrow sites such as the head (cranium, mandible), upper limb girdle (humerus, head and neck, scapulae, clavicles), sternum, ribs, vertebrae (cervical, thoracic, lumber, sacrum), and lower limb girdle (os coxae, femoral head and neck). PTV3 represents PTV2 with a 4 mm margin. This margin was selected based upon the accuracy of the kVCT-MVCT registration process. The contouring time currently averages about an hour but might decrease with greater experience or in some cases where special care is appropriate, it could take correspondingly more time. The optimization engine utilizes a quadratic objective function in which an iterative least-square minimization with soft constraints is applied.[39] The normal tissue dose constraints utilized were based on the results of the survey (presented in the Introduction) of the clinical outcome of the target dose and dose limits to various OARs.

The TomoTherapy Planning Station allows control over three delivery parameters for the planning process: field width, pitch, and modulation factor (MF). The field width is the full-width at half-maximum of the radiation field in the longitudinal (superior–inferior) direction. Similar to helical (spiral) CT, the pitch is defined as the ratio of the distance the couch travels per rotation to the field width (slice width) at the gantry axis. Finally, the MF is defined as the ratio of the maximum leaf opening time to the average opening time of all of the nonzero leaf opening times. A MF of unity means that the radiation intensity is not modulated (by keeping the leaves stationary).

A. TBI planning

A helical tomotherapy treatment plan for TBI was generated for the patient images and contours. The prescription (13.2 Gy, 1.65 Gy/fx, 8 fractions)[40] was used for planning simulation to cover PTV1 with the 95% isodose line. Maximum importance was given to the target dose coverage and homogeneity: soft constraints such as the minimum dose and penalty, maximum dose and penalty, and DVH dose and penalty were adjusted accordingly during optimization. To start the process, TERMA (Total Energy Released per unit MAss) iterations were performed in an effort to find the lowest MF and loosest pitch that maintained the DVH characteristics of a plan with high modulation and tight pitch. Such an approach allows the planner to attain the shorter delivery times for the same dose coverage. This effort resulted in a MF and pitch of 2.0 and 0.46, respectively.

Convolution/superposition dose distributions were then computed for all active leaves over all projections, where a single active leaf in a single projection is defined as one beamlet. For the 2.5 cm field width and a pitch of 0.46, there were 178 000 beamlets and the calculation time was 4.5 h. For the 5.0 cm field width and the same pitch, there were 90 000 beamlets and the calculation time was 2.75 h. Once the beamlet dose distributions were computed, the effects of changes in the soft constraint penalties could be rapidly visualized since the time per iteration was small (about 5 s). Typically, approximately 20 iterations are required to view the main impact of a change in constraint. We found a very small improvement in the dose coverage beyond 200 iterations. However, in this study we allowed optimization to proceed for all the planning up to approximately 1000 iterations (approximately 85 min).

The effect of variations in field width (2.5 and 5.0 cm), MF (2.0, 2.5, and 3.0) and pitch (0.46, 0.506, and 0.556) were simulated in detail by varying each physical parameter and keeping the two other parameters unchanged. The dose homogeneity index (DHI) of the target, dose statistics (maximum, minimum, and average dose), and dose DVH were generated from the planned histogram for each individual optimization calculation. The dose-homogeneity index (DHI) is used here to characterize the dose distributions, as reported by Mayo *et al.*[41] The DHI was defined as the ratio of the dose received by 90% of the volume to the minimum dose received by the "hottest" 10% of the volume.

B. TMI planning

In the second phase of the study, we simulated conformal total marrow irradiation (TMI) instead of TBI, as above. In this case, the treatment plan was simulated to confine the radiation dose (with higher importance) to either PTV2 or PTV3: bone marrow sites without and with a 4 mm margin, respectively. The planning optimization procedure was followed as before. All OAR soft constraints were kept unchanged. The effect of different field widths and a target margin were evaluated. For each individual optimization calculation, the cumulative DVH were analyzed for the target and for all OARs.

C. Rando TBI planning, setup, and delivery

To study the setup and delivery processes for such TBI treatments, a helical tomotherapy TBI plan was generated for a Rando phantom (The Phantom Laboratory, Salem, NY) that was 100 cm high. The same approach as described above was used in creating the plan. This resulted in a field width, pitch, and MF of 2.5 cm, 0.42, and 2.22, respectively. Once the plan was finished, setup and delivery were performed on the TomoTherapy HiArt system.

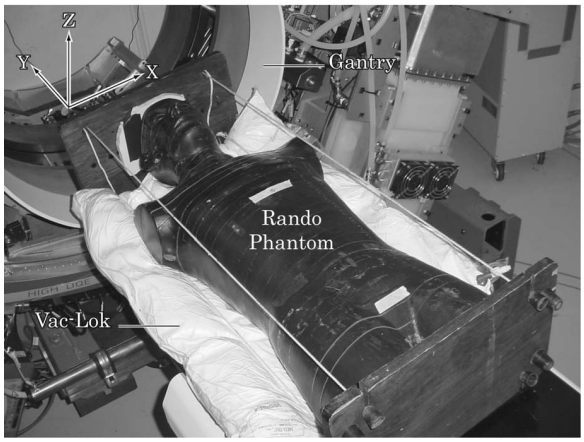

FIG. 1. Anthromorphic Rando phantom placed on a Vac-Lok bag as a part of treatment and imaging procedures. A point in the phantom is aligned at the virtual isocenter, which is located outside the bore of the gantry. The coordinate system is shown in the upper left corner. The gantry has its covers removed.

For setup, phantom localization was achieved by the following methods. A body immobilization device (Vac-Lok, MEDTEC, Orange City, IA) was used for the Rando phantom treatment, as shown in Fig. 1. The initial alignment of the red laser was on the kVCT marks (3 points in a line on the coronal section and 3 points in a line on the saggital section) with the phantom positioned at the virtual isocenter that is along the axis of rotation and displaced from the center of the beam plane by 70 cm so that the setup is done outside the gantry. Whole body megavoltage CT (MVCT) was performed using a normal mode (4 mm slice thickness). Automatic kVCT-MVCT fusions were performed based on the bony anatomy, soft tissue, and OAR outline. Occasionally, manual fusion was performed to improve the registration. This procedure was verified for transverse, coronal, and saggital views for each individual fusion study. In addition, limited MVCT (18–22 slices total) spread over sections of the head, chest, and pelvis were also measured several times to establish a quicker method of MVCT localization.[42,43]

To study the reproducibility of the setup process, the phantom was moved away from the couch, repositioned with the kVCT marks, and aligned with the laser at the virtual isocenter. These procedures were carried out several times to simulate a real patient situation. Translational coordinates (X, Y, and Z) and roll angle resulting from properly matched anatomy (after fusion) were used for setup verification and setup error analysis. The phantom and Vac-Lok were marked at the head, chest, and hip position once MVCT matched well with kVCT.

The TBI helical tomotherapy treatment required 31 min of beam-on time (for a field width of 2.5 cm) and was successfully performed with the Rando phantom fully instrumented for dose verification. We performed this procedure to test the machine capability to deliver a dose with sustained output for a longer run (without delivery fluctuation). However, with a 5.0 cm gantry field width, the treatment delivery time was approximately 16 min. For pediatric patients (an approximate height of 100 cm), the radiation dose delivery time will be similar to the Rando treatment time (16 min).

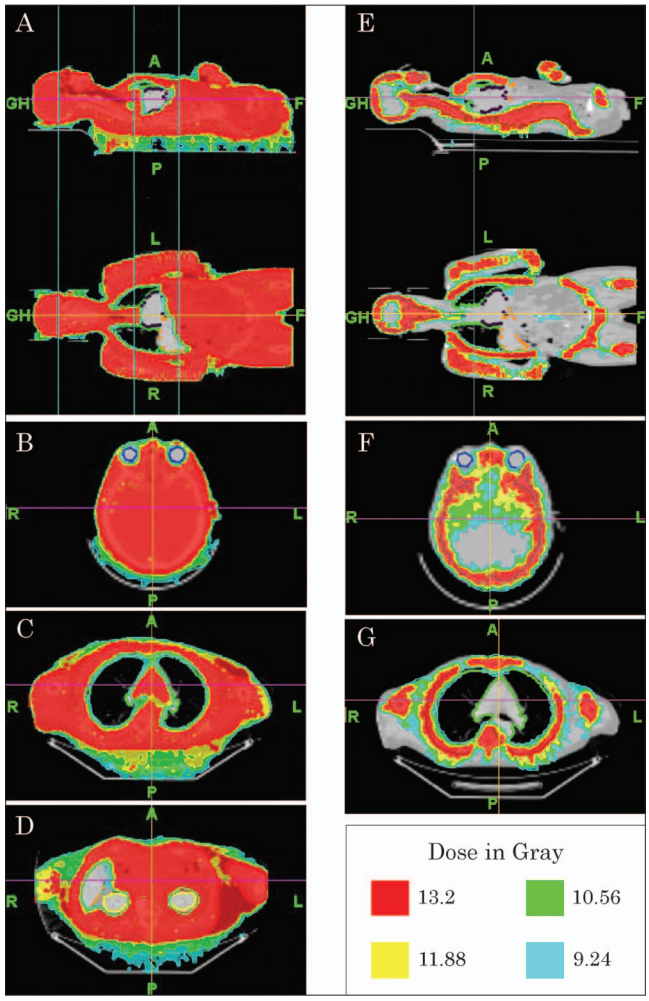

FIG. 2. Isodose distribution shown on a patient CT, as calculated by the tomotherapy treatment planning. The left-side [(A), (B), (C), (D)] panel shows the planning dose distribution for total body irradiation. The right-side [(E), (F), (G)] shows the planning dose distribution for total bone marrow irradiation. Planning was done with a 5.0 cm field width.

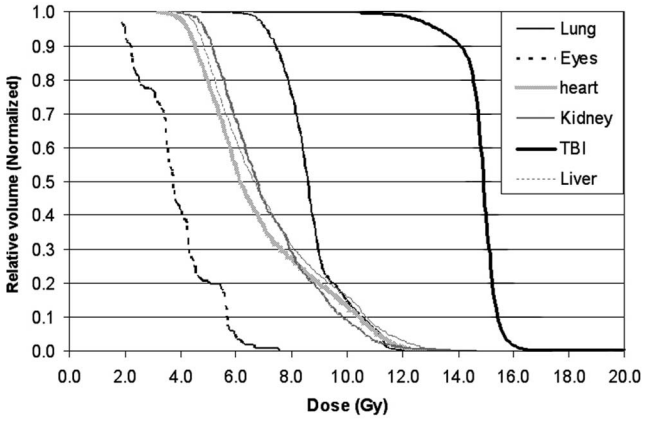

FIG. 3. Dose volume histogram for total body irradiation plan. Planning was done with 5.0 cm field width.

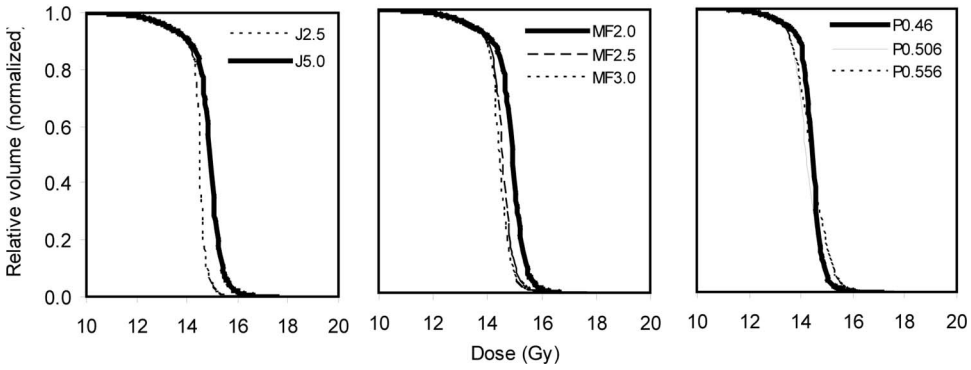

FIG. 4. The effect of field width (J), MF, and pitch (P) on DVH for total body irradiation shown from left to right, respectively. The dose scale is drawn from 10 to 20 Gy to amplify the DVH variations with J, MF, and P.

For adult patients, the height could be greater. In that case, the treatment time could increase by more than 50% (25 min). However, the actual treatment delivery length can be shortened (compared to physical height) by keeping the patient's legs in a folded position with a proper Vac-Lok for reproducibility. We measured the dose delivery three times in multiple areas using multiple LiF thermoluminescent dosimeters (TLD 100, powdered, 5% dose uncertainty) in capsules. TLDs were placed inside the Rando phantom at organ sites of interest, such as manubrium, lung, xyphoid, iliac crest, and hip. The TLDs were calibrated and tested for linearity with respect to the dose for a range from 50 to 500 cGy. The dose result was derived by averaging all measurements. The standard deviation (STD) was calculated to estimate the spread of the planned data relative to the average value where the average was taken over multiple points in the same volumetric structure.

V. RESULTS

A. Total body irradiation plan

The dose coverage to the whole body is shown in a color wash presentation in Figures 2(a)–2(d) for a treatment planning simulation with field width; the pitch and MF of 5.0, 0.46, and 2.0, respectively. Three levels of transverse images for sensitive structures are shown: eyes (B), lungs (C), kidneys and liver (D).

The dose reduction to various OARs relative to conventional TBI varied from 34%–70%. A DVH for this plan is shown in Fig. 3. The 95% isodose surface (12.54 Gy) covers 95% of the PTV and the DHI of the PTV was within ±10%. The significant reduction relative to conventional TBI (dose levels for various OARs were discussed above) is clear in the DVH plot. Figure 4 and Tables I, II, and III illustrate that further improvements, albeit small, can be attained for helical tomotherapy plans through a variation of the field width, MF, and pitch. Target dose homogeneity improves with a smaller field width (*J*) and higher MF, as shown in Fig. 4.

1. Field width effect

In both field sizes, the 95% isodose line covers the target adequately. However, dose homogeneity was improved by a small amount (3%) with a 2.5 cm field with very small variation (2%–3%) in the average dose to the target. The average dose coverage (for a total of eight fractions) for different organs with variations in field width is shown in Table I. This was the case when the pitch and MF were kept invariant. The treatment delivery time with a 5.0 cm field width was about 15 min compared to 31 min for a 2.5 cm field width when the pitch and MF were 0.46 and 2.0, respectively. With a 2.5 field width, the dose reduction that was achieved for critical tissues varied from 1% (lung) to almost 22% (heart) compared to a 5 cm field width (Table I).

2. Modulation factor effect

The DHI decreased 2%, implying slightly greater homogeneity, with the increase in MF from 2 to 2.5 (Table II). However, the DHI did not vary with MF and increased from 2.5 to 3.0. Higher modulation lowered the average critical tissue doses. However, MF 2.0 still offered average dose levels that were below the toxicity limit for each organ. A 5%–10% reduction in the average dose was observed for critical tissues when changing the MF from 2.0 to 2.5, at the expense of a 25% increase in delivery time, which is directly proportional to MF. The highest MF studied, 3.0, increased

TABLE I. Average dose coverage (for total 8 fractions, 1.65 Gy/fx) for different organs with variations in field width (MF 2.0 and pitch 0.46).

Field width (cm)	DHI	Average Dose (Gy)					
		Total body	Lungs	Eyes	Kidneys	Liver	Heart
2.5	0.94	14.35	8.6	3.19	6.33	6.19	5.32
5	0.91	14.78	8.72	3.88	7.15	7.24	6.82

TABLE II. Average dose coverage (for total 8 fraction, 1.65 Gy/fx) and impact of MF on the average dose in various OARs and target (field width 5 cm and pitch 0.46).

Anatomy	Average dose (Gy)	% reduction in average dose	
	(MF 2.0)	(MF 2.5)	(MF 3.0)
Total body	14.78	2	4
Lungs	8.72	6	14
Eyes	3.88	5	6
Kidneys	7.15	8	9
Heart	6.82	14	21
Liver	7.24	12	15
DHI	0.91	0.93	0.93

delivery time by 50% as compared to a MF of 2.0. The reduction in the average dose was more pronounced for the lungs and heart.

3. Pitch effect

A higher pitch did not significantly change homogeneity. The DHI worsened by 2% with every 10% change (loosening) in pitch from 0.46 to 0.556. The average dose coverage and impact of pitch on the average dose in various OARs and the target is shown in Table III. The higher pitch values had variable effects on the average dose to the critical tissues: in some cases the average dose was reduced while in others it increased. For both cases, the changes were not significantly large (+6.0% being the largest change observed). This amount of variation did not greatly impact dose statistics such as the average, maximum, and minimum dose.

B. Total marrow irradiation plan

Highly conformal dose coverage to the bone marrow sites was achieved, as shown in Figs. 2(e)–2(g) and Fig. 5 when marrow was deliberately targeted instead of total body irradiation. The dose distribution to the target and OARs are shown in Figs. 2(e)–2(g): two transverse [2(f) and 2(g)] sections (eyes and lungs), saggital, and coronal (upper and lower E) kVCT with the dose in color wash. The detailed

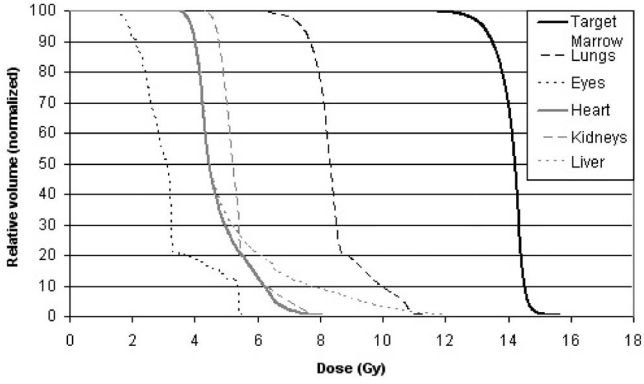

FIG. 5. Dose volume histogram for the total marrow irradiation plan. Planning was done with a 5.0 cm field width. The marrow target included a 4 mm margin.

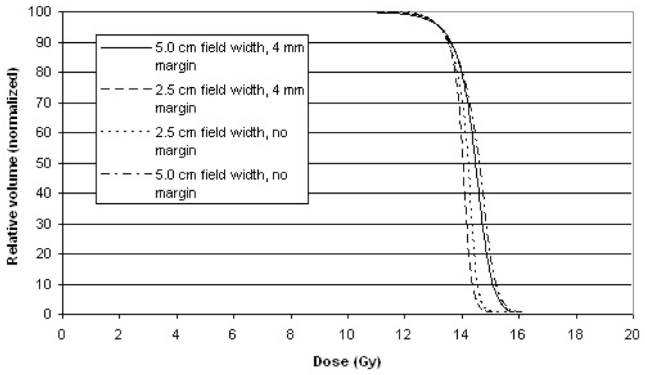

FIG. 6. Dose volume histogram for a total marrow target using the 5.0 cm and 2.5 cm field width, with and without a 4 mm margin. Higher conformality is obtained with the 2.5 cm field width.

DVH to the target bone marrow is shown in Fig. 5. The effect of the field width (2.5 and 5.0) and the margin on the target is shown in Fig. 6. The addition of a margin slightly degrades homogeneity for both field widths. The average doses to lungs, kidneys, heart, and eyes were reduced by 40%–60% compared to the prescribed dose for TMI treatments (Fig. 7).

C. Rando TBI setup, delivery, and verification

1. MVCT image localization and setup verification

Megavoltage (MVCT) images were obtained in the normal scanning mode (4 mm slice thickness) for the whole body via helical tomotherapy [Fig. 8(a)]. A limited MVCT scan for the head (level I), chest (level II) and pelvis (level III) were also fused with kVCT, as shown in Fig. 8(b). Based on the bony anatomy, soft tissue, and outline of critical structures, MVCT was automatically fused[36] with kVCT, as shown in Fig. 8(a) and Fig. 8(b). The fusion results were then verified manually using transverse, saggital, and coronal views. We show here a comparative study of MVCT and limited MVCT and fusion for coronal, saggital, and transverse views, respectively [Figs. 8(c)–8(f)].

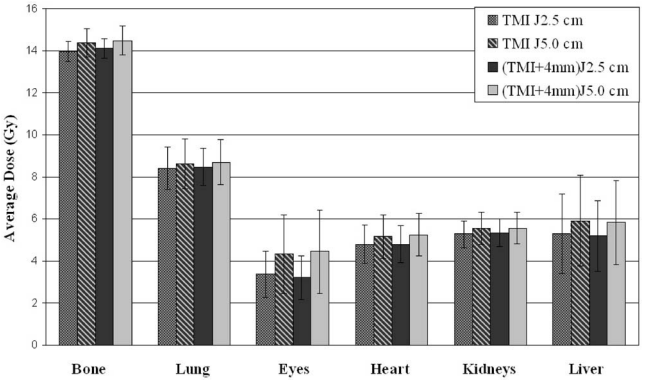

FIG. 7. Bar chart shown for bone target and critical organs—lungs, eyes, heart, kidneys, and liver. Four bars in each group represents the average dose for 2.5 and 5.0 cm field width for bone marrow only and bone marrow +4 mm margin with standard deviation as an uncertainty.

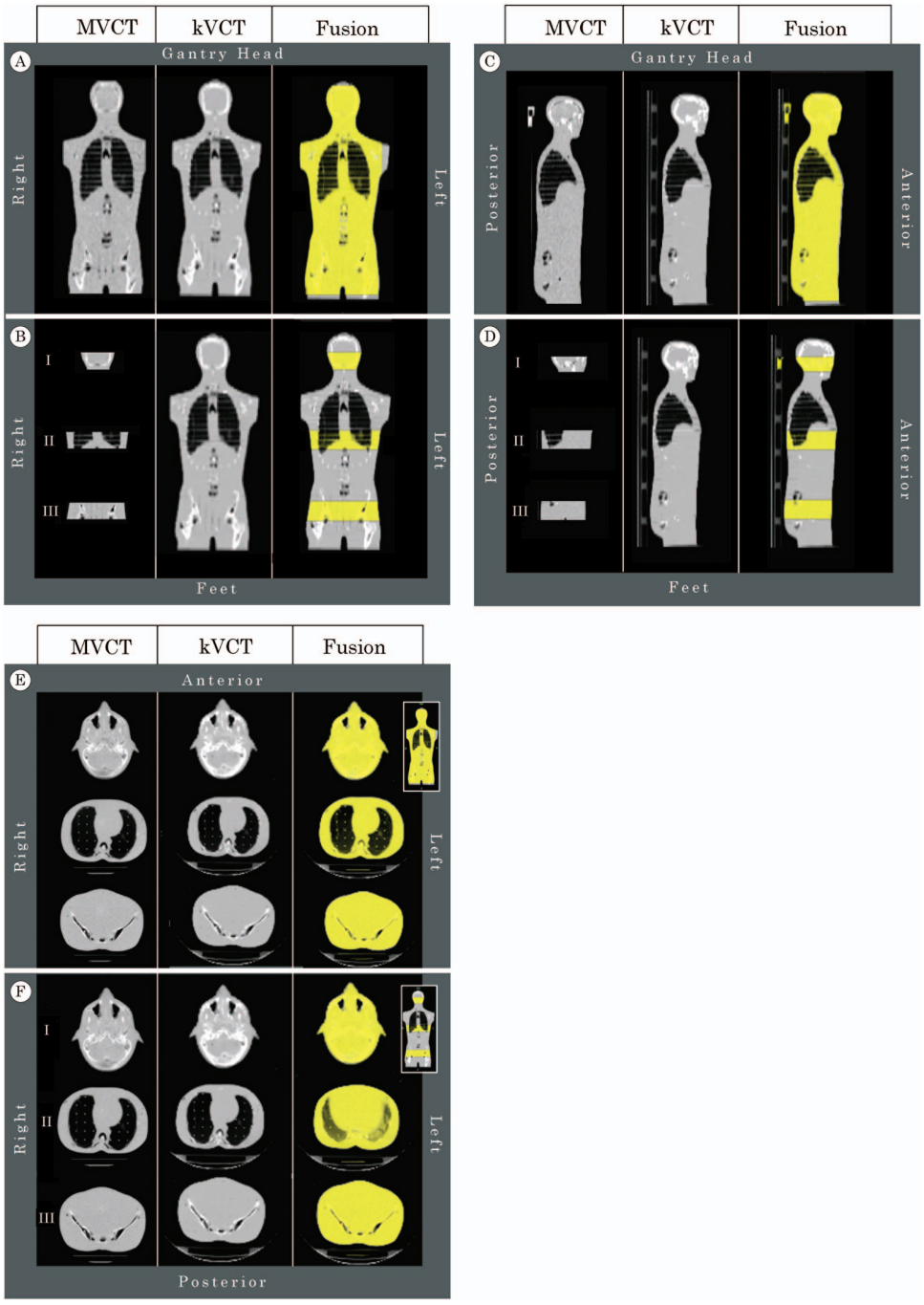

FIG. 8. (A) Whole body MVCT, treatment planning kVCT, and fused images in a coronal view. (B) Limited MVCT at the level of (I) head, (II) chest, and (III) pelvis; treatment planning kVCT; and fused images in a coronal view. The saggital sectional view is shown in (C) and (D), and the transverse sectional view is shown in (E) and (F). For each panel, the fusion column presents the kVCT in gray scale with the MVCT superimposed with a level of transparency in yellow.

Shifts in coordinates (translational coordinates and roll) derived from fusion between MVCT and kVCT were used for localization of the Rando. The average shifts in coordinates (after fusion) for whole body and limited MVCT are tabulated in Table IV. The time required for whole body MVCT and limited MVCT were 13 and 5.25 min, respectively.

2. Dose verification

The CT-based treatment plan dose was compared with the average TLD measurement. This is shown in Table V. The average anatomical doses to hip, umbilicus, xiphoid, manubrium, head, and lungs were measured by TLDs. Readings for all the verification points were within the uncertainty of the average readings of the TBI planned dose. The right and left lung doses were reduced by 50% relative to the conventional lateral TBI[32] as calculated by the tomotherapy planning. This was confirmed by TLD readings.

VI. DISCUSSION

In this investigation we demonstrate that the helical tomotherapy reduces the dose significantly to all critical organs, including lungs without the necessity of special procedures (external blocks and/or compensators) required for shielding each individual critical organ. The radiation dose to the lungs was reduced compared to the prescribed dose, and full dose

TABLE III. Average dose coverage (for total 8 fraction, 1.65 Gy/fx) and impact of pitch on average dose in various OARs and target (field width 5 cm and MF 3.0). Note: −ve means reduction and +ve means increment in percentage mean dose in eight fractions.

Anatomy	Average dose (Gy)	% variation in average dose	
	Pitch 0.46	Pitch 0.506	Pitch 0.556
Total body	14.34	−1	0
Lungs	7.84	−4	−1
Eyes	3.63	0	−1
Kidneys	6.35	2	6
Heart	5.65	−3	2
Liver	6.05	2	3
DHI	0.93	0.91	0.89

TABLE V. Doses measured with TLD compared to prescribed doses at the selected points in the rando phantom irradiated with helical tomotherapy for a single fraction 1.65 Gy. The uncertainty in TLD reading (radiation dose measurement) was 5%.

Anatomy	Average dose (Gy)/fraction	
	TLD reading (uncertainty)	Planning (STD)
Head	1.62(±0.08)	
Manubrium	1.68(±0.03)	1.74(±0.05)
Xyphoid	1.68(±0.08)	
Umbilical	1.68(±0.08)	
Hip	1.68(±0.08)	
Rt lung	0.89(±0.04)	0.89(±0.09)
Lt lung	0.92(±0.04)	0.93(±0.09)

coverage was retained in marrow regions (e.g., ribs, sternum) that may be compromised with lung blocks in conventional TBI,[32] resulting in a high incidence of relapse.[33] A variation in relative lung and arm size, and daily variation in arm placement during treatment can lead to variations in the dose distribution and failure to adequately shield the lungs.[32] Sometimes an electron beam boost (in an AP/PA technique) is used to compensate dose reduction to the ribs and manubrium but adds complexity, uncertainty, and additional time to the treatment. Even with a special procedure to achieve better homogeneity in the AP/PA technique, Thomas *et al.*[44] observed a statistically higher pulmonary complication compared to the lateral treatment positions. Moreover, it is difficult to assess the limiting lung dose from the single-point dose calculation model generally used in the grossly inhomogeneous dose distribution within the lungs. The dose volume histograms generated from the tomotherapy treatment planning could be very useful for maintaining dose homogeneity with lung shielding and accurate dose coverage to nearby bone (i.e., ribs, manubrium).

As another example, this approach may be advantageous in reducing radiation-related orbital complications (i.e., cataracts).[14–16] At present, no TBI method is available to reduce the dose to the eyes without reducing the entire orbit dose. In addition to homogeneous dose coverage to the total body target including the rest of the orbit, our treatment method reduced the dose to the eyes (and all OARs) to subthreshold doses [Fig. 2(b)] a for complications and offered dose-volume histograms that might be useful for a future correlation with clinical outcomes (Fig. 3). Tomotherapy treatment planning achieved a similar dose reduction to other critical organs such as the kidneys and liver.

TABLE IV. A comparison of the lateral (Tx), longitudinal (Ty), and vertical (Tz) (IEC nomenclature) and roll offsets resulting from fusion for the average of the limited MVCT (fifth row) and whole body MVCT (last row). The uncertainties for the average values were obtained by adding the individual uncertainties in quadrature.

Anatomy	Tx (mm)	Ty (mm)	Tz (mm)	Roll (degrees)
Head	1.83	0.63	−3.43	−1.22
Chest	0.98	−1.28	−0.21	0.32
Hip	0.39	−1.68	0.75	1.30
Average	1.06	−0.78	−0.96	0.13
(uncertainty)	(2.11)	(2.20)	(3.52)	(1.81)
Total body	−0.22	3.08	1.61	0.61

The understanding of the influence of each individual physical parameters (field width, pitch, MF) is essential to improve target dose coverage, critical tissue dose, and delivery time. The feasibility of such improvements is another advantage of the use of helical tomotherapy in TBI. In general, smaller field widths, tighter pitch values, and/or large MFs can result in more effective plans due to the greater control in the superior–inferior direction (field width), more opportunities to "see" targets from many angles (pitch), and a greater allowance for widely disparate leaf opening times between projections (modulation factor). However, the reduction of critical organ doses with the use of a 2.5 cm field width may not be as clinically relevant as the possibility of reducing the treatment time by 50% with a 5.0 cm field width. In both cases the doses to all critical organs were below the threshold for complications, thus the treatment time may be a practical consideration in a busy clinic. On the other hand, the advantages of the 2.5 cm field width may be preferable in pediatric patients due to the smaller target length, which leads to shorter treatment times. In general, a MF of 2.0 generates reasonable DVHs for both target and critical organs. However, MF variation might be an option to consider if a further reduction of the critical organ dose (by 5%–10%, depending on the location, volume) is necessary. Over the small range of pitch change (10% and 20% higher) studied here, it is difficult to draw generalities based on the data obtained (such as that in Table III). This is not problematic but rather a statement that for the pitch range studied, the delivery helix changed in such a manner that did not significantly impact the average dose values. Put another way, the optimization process was able to still find leaves for beam angles that allow for a homogeneous target dose while limiting the dose to OARs. Unlike standard TBI treatment (where the beam incidence is at normal to the skin surface), the tomotherapy dose to the buildup and surface (skin) region was adequately covered. This was possible for two ma-

jor reasons: (a) the oblique incidence of beamlets from a rotational beam (360° rotations) increases the dose to the buildup region and surface.[45] (b) The modulation of beam intensity additionally helps in retaining dose homogeneity in that region.

Selective conformal irradiation of the bone marrow[46] was achieved with a reduction of the dose to nonhematopoetic tissues including the OARs [Figs. 2(e)–2(g) and 5, 6, and 7]. This outcome was also verified with a safe margin for the target. This conformal targeted irradiation procedure may be useful for accelerated TBI and/or an alternative to radiolabeled antibody therapy[47] without increasing normal tissue toxicity. The targeted external irradiation eliminates the prolonged hospitalization required for radiolabeled antibody treatment and also reduces the renal dose. This approach to TBI might be useful for nonmalignant applications or for safely escalating the dose in high-risk leukemia patients. Hawkins *et al.*[48] showed the usefulness of total marrow irradiation in poor risk Ewing sarcoma family tumors (ESFT). However, in their treatment procedure, they essentially treated bone marrow using TBI while blocking the lungs and liver only. Advantages of our proposed TMI technique are (a) the radiation dose can be delivered to the specific target bone (bone marrow), (b) the radiation dose to healthy tissue of the whole body can be reduced, (c) in addition to the lung and liver, radiation dose reductions to all other critical organs (e.g., eyes, kidneys) are achievable without external blocking procedures. Relapse is a major concern for bone marrow transplant procedures.[49,50] Given the relative radiosensitivity of hematological malignancies, the dose escalation may be valuable for improving relapse-free survival for high risk patients. Both TBI and TMI methods can be used to enhance dose to the target while keeping OAR doses below the threshold. Increasing the radiation dose by 2 Gy (BED equivalent of 15% enhancement) or 3 Gy (BED equivalent of 25% enhancement) while keeping the dose to OARs below toxicity thresholds now appears to be a feasible option with this approach.

There are several publications without any adverse effects of the high dose rate on total body radiation.[51–57] The dose rate has been shown to have very little adverse effect once fractionated regimes were used.[53] In fact, an increased dose rate can be beneficial for successful bone engraftment for those cases where malignant cells are radiosensitive.[51,54,55] However, other reports have suggested that the high dose rate may have adverse effects on normal organs.[58,59] It is prudent to be extremely cautious with the dose rate issue before clinical implementation. Proper patient selection for clinical evaluation may lead to a better understanding of radiobiology and a clinical outcome. One approach would be to find cases where the relapse rate is quite high (45%) (e.g. Ewing sarcoma, Rhabdomyosarcoma, etc.).[48] These high risk patients relapsed mainly in bony sites, presumably due to areas of micrometastatic disease that were resistant to the conditioning chemotherapy.

Although most of the clinics followed the common TBI treatment methods, as described in the AAPM report,[29] sequential TBI treatment methods[56–58] were developed to overcome limitations of smaller room and extended setup procedures that lead to an interruption of daily treatment. Examples of these techniques are the translational bed technique,[56] sweeping beam,[57] and sequential half-body irradiation[60] methods and patients underwent safe treatment without reported adverse effects. This evidence provides logical support to the helical tomotherapy sequential treatment method. The concern of circulating malignant cells is not likely to be important since patients with detectable malignant cells in the circulation are excluded from our TBI protocols. In fact, many patients are treated when they are in the remission phase, at a time when they do not have any active disease. In general, the circulation of malignant cells in the peripheral blood and lymphatic circulation is expected to be extremely infrequent. Thus the significance of this issue as it relates to Tomotherapy TBI/TMI is impossible to determine at this stage and must be addressed in additional studies.

One of the essential requirements of conformal external beam radiation therapy is target localization to reduce the possibility of underdosing (cold spot) the target.[61] Confirmation of the relative position and shape of the target and organs at risk during daily treatment is essential for accurate dose delivery.[37] The MVCT 3D imaging capability reduces the uncertainty of daily positioning of the anatomy at the time of delivery by acquiring volumetric images and fusing those images with pretreatment kVCT images.[36,37] This uncertainty in Rando localization was included in a TMI planning optimization calculation. Further avenues of inquiry might include a clinical evaluation of MVCT localization uncertainty on human subjects. In most applications of radiation therapy, the tumor is localized within a small area, and hence the time requirement for MVCT is small; however, MVCT for the whole body requires a much longer time. The limited MVCT method (MVCT sampling of head, chest, and pelvis) seems an effective and efficient way to reduce the patient setup verification time for daily treatment. This may have importance for clinical application since the patient has to tolerate a long treatment time. In addition, the limited MVCT method spared most parts of the body from unnecessary radiation from imaging. However, the time required for a limited MVCT may vary with the number of slices selected to be scanned and mode of scanning (e.g., fine, normal, or coarse). In a future development, this procedure could be automated for a further reduction of imaging time. In addition, the incorporation of four-dimensional (4D) breathing motion in tomotherapy treatment optimization and synchronized treatment delivery will further improve the radiation delivery accuracy, as reported by Zhang *et al.*[62] However, this is not available for clinical use yet.

Last, for clinicians to be confident in the actual treatment, there must be confidence in the accuracy of the planning dose presented by the treatment planning system. This was successfully confirmed by TLD measurements (Table V). In selecting the areas for TLD placement, we sought to verify the dose from two key aspects of delivery: (1) Areas significantly affected by inhomogeneities. (2) Output consistency over the entire 31 min treatment. The former was verified by

the accuracy of the lung TLD measurements. The latter was verified by the collective accuracy of all TLD measurements from the start of the delivery (e.g., TLDs in the head region) to the end (e.g., TLDs in the hip).

VII. CONCLUSION

Novel approaches to total body irradiation and total marrow irradiation treatment have been proposed using helical tomotherapy, which offers the possibility of many attractive advantages over conventional methods of treatment. In a preclinical feasibility study, helical tomotherapy treatment planning simulation shows homogeneous dose coverage to the total body target. In addition to lung, substantial radiation dose reductions to all sensitive structures are possible with this new technique of intensity modulated radiation therapy. The basic beam dosimetry has been reviewed and the physical factors producing dose variation have been evaluated. The volumetric dosimetry obtained from this method and outcomes of future clinical trials will be important for further dosimetric optimization of these new techniques. In external radiation therapy, conformal radiation to the bone marrow (total marrow irradiation) appears to be feasible, with a substantial dose reduction to all normal healthy tissues, including critical organs. The treatment planning system and tomotherapy machine offer the flexibility to tailor the treatment delivery within a reasonable amount of time. In addition, MVCT image guidance offers effective setup verification in clinically acceptable time frames and helps to increase accuracy of the dose delivery.

ACKNOWLEDGMENTS

We would like to thank Dr. Michael Verneris, Dr. Rupak Das, Dr. Seymour Levitt, Dr. Bruce Thomadsen, Dr. Bhudatt Paliwal, Dr. Minesh Mehta, and Dr. Kathryn Dusenbery for their helpful discussion. We would like to thank Tiffany J Glass for assisting in figure preparation. The authors associated with TomoTherapy Inc. have a financial interest in that company. This work was partially supported by NCI grant P01 CA088960.

[a)]This work was initiated at the University of Wisconsin, Madison.
[b)]Address for correspondence: Susanta K. Hui, Department of Therapeutic Radiology, University of Minnesota, 420 Delaware Street SE, Mayo Mail Code 494, Minneapolis, Minnesota 55455. Phone: 612-626-4484; fax: 612-626-7060; electronic mail: huixx019@umn.edu

[1]B. Sabine, H. Claudine, C. Bernard, and M. Raymond, "Total body irradiation before allogeneic bone marrow transplantation: is more dose better?," Int. J. Radiat. Oncol., Biol., Phys. **49**, 1071–1077 (2001).
[2]G. Socie *et al.*, "Influence of the fractionation of total body irradiation on complication and relapse rate for chronic myelogenous leukaemia," Int. J. Radiat. Oncol., Biol., Phys. **20**, 397–404 (1991).
[3]T. L. Morgan, P. M. Falk, N. Kogut, K. H. Shah, M. Tome, and A. R. Kagan, "A comparison of single dose and fractionated total-body irradiation on the development of pneumonitis following bone marrow transplantation," Int. J. Radiat. Oncol., Biol., Phys. **36**, 61–66 (1996).
[4]J. M. Cosset, G. Socie, B. Dubray, T. Girinsky, A. Fourquet, and E. Gluckman, "Single dose versus fractionated total body irradiation before bone marrow transplantation: Radiobiological and clinical consideration," Int. J. Radiat. Oncol., Biol., Phys. **30**, 477–492 (1994).
[5]D. Scarpati, F. Frassoni, V. Vitale, R. Corvo, P. Franzone, S. Barra, M. Guenzi, and M. Orsatti, "Total body irradiation in acute myeloid leukemia relapse," Int. J. Radiat. Oncol., Biol., Phys. **17**, 547–552 (1989).
[6]A. D. Volpe, A. J. M. Ferreri, C. Annaloro, P. Mangili, A. Rosso, R. Calandrino, E. Villa, G. Lambertenghi-Deliliers, and C. Fiorino, "Lethal pulmonary complications significantly correlate with individual assessed mean lung dose in patients with hematologic malignancies treated with total body irradiation," Int. J. Radiat. Oncol., Biol., Phys. **52**, 483–488 (2002).
[7]Z. Weshler, R. Breuer, R. Or, E. Naparstek, M. R. Pfeffer, E. Lowental, and S. Slavin, "Interstitial pneumonitis after total body irradiation: Effects of total lung shielding," Br. J. Haematol. **74**, 61–64 (1990).
[8]A. Barrett, "Relationship of irradiation to pulmonary complications," Exp. Hematol. **12**, 67 (1984).
[9]T. J. Keane, J. Van Dyk, and W. Rider, "Idiopathic interstitial pneumonia following bone marrow transplantation: the relationship with total body irradiation," Int. J. Radiat. Oncol., Biol., Phys. **7**, 1365–1370 (1981).
[10]R. C. Tait, A. K. Burnett, A. G. Robertson, S. McNee, B. M. Riyami, R. Carter, and R. D. Stevenson, "Subclinical pulmonary function defects following autologous and allogeneic bone marrow transplantation: Relationship to total body irradiation and graft versus-host-disease," Int. J. Radiat. Oncol., Biol., Phys. **20**, 1219–1227 (1991).
[11]B. Bruno, G. Souillet, Y. Bertrand, M. C. Werck-Gallois, A. So Satta, and G. Bellon, "Effects of allogeneic bone marrow transplantation on pulmonary function in 80 children in a single paediatric centre," Bone Marrow Transplant **34**, 143–147 (2004).
[12]D. G. Cogan, D. D. Donaldson, and A. B. Reese, "Clinical and pathological characteristics of radiation cataract," AMA Arch. Ophthalmol. **47**, 55–70 (1952).
[13]M. L. van Kempen-Harteveld, Y. Belkacémi, H. B. Kal, M. Labopin, and F. Frassoni, "Dose-effect relationship for cataract induction after single-dose total body irradiation and bone marrow transplantation for acute leukemia," Int. J. Radiat. Oncol., Biol., Phys. **52**, 1367–1374 (2002).
[14]Y. Belkacemi, M. Ozsahin, F. Pene, B. Rio, J. P. Laporte, V. Leblond, E. Touboul, M. Schlienger, N. C. Gorin, and A. Laugier, "Cataractogenesis after total body irradiation," Int. J. Radiat. Oncol., Biol., Phys. **35**, 53–60 (1996).
[15]D. L. Cooper, S. Seropian, and R. W. Childs, "Autologous and allogeneic stem cell transplant," in *Cancer: Principles and Practice of Oncology*, 6th ed., edited by V. T. DeVita, S. Hellman, and S. A. Rosenberg (Lippincott, Williams & Wilkins, Philadelpia, 2001), pp. 2773–2798.
[16]J. R. Cassady, "Clinical radiation nephropathy," Int. J. Radiat. Oncol., Biol., Phys. **31**, 1249–1256 (1995).
[17]P. Rubin and G. W. Casarett, *Clinical Radiation Pathology* (Saunders, Philadelphia, 1968), Vols. 1 and 2.
[18]R. Miralbell, G. Sancho, S. Bieri, I. Carrio, C. Helg, S. Brunet, P. Y. Martin, A. Sureda, G. Gomez De Segura, B. Chapuis, M. Estorch, M. Ozsahin, and A. Keller, "Renal insufficiency in patients with hematologic malignancies undergoing total body irradiation and bone marrow transplantation: a prospective assessment," Int. J. Radiat. Oncol., Biol., Phys. **58**, 809–1816 (2004).
[19]C. A. Lawton, E. P. Cohen, K. J. Murray, S. W. Derus, J. T. Casper, W. R. Drobyski, M. M. Horowitz, and J. E. Moulder, "Long-term results of selective renal shielding in patients undergoing total body irradiation in preparation for bone marrow transplantation," Bone Marrow Transplant **20**, 1069–1074 (1997).
[20]M. Hassan, P. Ljungman, O. Ringden, Z. Hassan, G. Oberg, C. Nilsson, A. Bekassy, M. Bielenstein, M. Abdel-Rehim, S. Georen, and L. Astner, "The effect of busulphan on the pharmacokinetics of cyclophosphamide and its 4-hydroxy metabolite: time interval influence on therapeutic efficacy and therapy-related toxicity," Bone Marrow Transplant **25**, 915–924 (2000).
[21]J. H. Lee, K. H. Lee, S. J. Choi, Y. J. Min, J. G. Kim, S. Kim, J. S. Lee, S. H. Kim, C. J. Park, H. S. Chi, and W. K. Kim, "Veno-occlusive disease of the liver after allogeneic bone marrow transplantation for severe aplastic anemia," Bone Marrow Transplant **26**, 657–662 (2000).
[22]T. Girinsky, E. Benhamou, J. H. Bourhis, F. Dhermain, D. Guillot-Valls, V. Ganansia, M. Luboinski, A. Perez, J. M. Cosset, G. Socie, D. Baume, N. Bouaouina, E. Briot, A. Beaudre, A. Bridier, and J. L. Pico, "Prospective randomized comparison of single-dose versus hyperfractionated total-body irradiation in patients with hematologic malignancies," J. Clin. Oncol. **18**, 981–986 (2000).
[23]T. Murdych and D. J. Weisdorf, "Serious cardiac complications during bone marrow transplantation at the University of Minnesota, 1977–1997," Bone Marrow Transplant **28**, 283–287 (2001).

[24]L. M. Buja, V. J. Ferrans, and R. G. Graw, Jr., "Cardiac pathologic findings in patients treated with bone marrow transplantation," Hum. Pathol. **7**, 17–45 (1976).
[25]W. Blum, H. Khoury, H. S. Lin, R. Vij, L. T. Goodnough, S. Devine, J. Dipersio, and D. Adkins, "Primary amyloidosis patients with significant organ dysfunction tolerate autologous transplantation after conditioning with single-dose total body irradiation alone: A feasibility study," Biol. Blood Marrow Transplant **9**, 397–404 (2003).
[26]J. R. Cunningham and D. J. Wright, "A simple facility for whole body irradiation," Radiology **78**, 941–949 (1962).
[27]C. S. Chui *et al.*, "Total body irradiation with an arc and a gravity-oriented compensator," Int. J. Radiat. Oncol., Biol., Phys. **39**, 1191–1195 (1997).
[28]M. Pla, S. G. Chenery, and E. B. Podgorsak, "Total body irradiation with a sweeping beam," Int. J. Radiat. Oncol., Biol., Phys. **9**, 83–89 (1983).
[29]AAPM (American Association of Physicists in Medicine. "The physical aspects of Total and Half Body photon Irradiation," in AAPM Report No. 17, Chairman: J. Van Dyk, American Institute of Physics, New York, 1986.
[30]B. J. Gerbi and K. E. Dusenbery, "Design specifications for a treatment stand used for total body photon irradiation with patients in a standing position," Med. Dosim **20**, 25–30 (1995).
[31]T. E. Wheldon, "The radiological basis of total body irradiation," Br. J. Radiol. **70**, 1204–1207 (1997); G. G. Steel and T. E. Wheldon, "The radiation biology of paediatric tumours," in *Paediatric Oncology*, edited by R. Pinkerton and N. Plowman (Wiley, London, 1991).
[32]S. K. Hui, D. Henderson, R. K. Das, and B. Thomadsen, "CT based analysis of dose homogeneity in total body irradiation using lateral beam," J. Appl. Clin. Med. Phys. **5**, 1–9 (2004).
[33]J. E. Anderson, F. R. Appelbaum, G. Schoch, T. Barnett, T. R. Chauncey, M. E. Flowers, and R. Storb, "Relapse after allogeneic bone marrow transplantation for refractory anemia is increased by shielding lungs and liver during total body irradiation," Biol. Blood Marrow Transplant **7**, 163–170 (2001).
[34]L. L. van Kempen-Harteveld, M. H. van Weel-Sipman, C. Emmens, E. M. Noordijk, I. van der Tweel, T. Revesz, H. Struikmans, H. B. Kal, A. van der Does-van den Berg, and J. M. Vossen, "Eye shielding during total body irradiation for bone marrow transplantation in children transplanted for a hematological disorder: Risks and benefits," Bone Marrow Transplant **31**, 1151–1156 (2003).
[35]G. H. Olivera, D. M. Shepard, P. J. Reckwerdt, K. Ruchala, J. Zachman, E. E. Fitchard, and T. R. Mackie, "Maximum likelihood as a common computational framework in tomotherapy," Phys. Med. Biol. **43**, 3277–3294 (1998).
[36]J. S. Welsh, R. R. Patel, M. A. Ritter, P. Harari, T. R. Mackie, and M. P. Mehta, "Helical Tomotherapy: An Innovative Technology and Approach to Radiation Therapy," Technology in Cancer Research and Treatment **1**, 55–63 (2002).
[37]T. R. Mackie, J. Kapatoes, K. Ruchala, W. Lu, C. Wu, G. Olivera, L. Forrest, W. Tome, J. Welsh, R. Jeraj, P. Harari, P. Reckwerdt, B. Paliwal, M. Ritter, H. Keller, J. Fowler, and M. Mehta, "Image guidance for precise conformal radiotherapy," Int. J. Radiat. Oncol., Biol., Phys. **56**, 89–105 (2003).
[38]J. M. Kapatoes, G. H. Olivera, K. J. Ruchala, J. B. Smilowitz, P. J. Reckwerdt, and T. R. Mackie, "A feasible method for clinical delivery verification and dose reconstruction in tomotherapy," Med. Phys. **28**, 528–542 (2001).
[39]D. M. Shepard, G. H. Olivera, P. J. Reckwerdt, and T. R. Mackie, "Iterative approaches to dose optimization in tomotherapy," Phys. Med. Biol. **45**, 69–90 (2000).
[40]K. E. Dusenbery, M. Steinbuch, P. B. McGlave, N. K. Ramsay, B. R. Blazar, J. P. Neglia, C. Litz, J. H. Kersey, and W. G. Woods, "Autologous bone marrow transplantation in acute myeloid leukemia: The University of Minnesota experience," Int. J. Radiat. Oncol., Biol., Phys. **36**, 335–343 (1996).
[41]C. S. Mayo and M. M. Urie, "A systematic benchmark method for analysis and comparison of IMRT treatment planning algorithms," Med. Dosim **28**, 235–242 (2003).
[42]K. J. Ruchala, G. H. Olivera, J. M. Kapatoes, E. A. Schloesser, P. J. Reckwerdt, and T. R. Mackie, "Megavoltage CT image reconstruction during tomotherapy treatments," Phys. Med. Biol. **45**, 3545–3562 (2000).
[43]J. S. Welsh, K. Bradley, K. J. Ruchala, T. R. Mackie, R. Manon, R. Patel, P. Wiederholt, M. Lock, S. Hui, and M. P. Mehta, "Megavoltage computed tomography imaging: a potential tool to guide and improve the delivery of thoracic radiation therapy," Clin Lung Cancer **5**, 303–306 (2004).
[44]O. Thomas, M. Mahe, L. Campion, S. Bourdin, N. Milpied, G. Brunet, A. Lisbona, A. Le Mevel, P. Moreau, J. Harousseau, and J. Cuilliere, "Long-term complications of total body irradiation in adults," Int. J. Radiat. Oncol., Biol., Phys. **49**, 125–131 (2001).
[45]B. J. Gerbi, A. S. Meigooni, and F. M. Khan, "Dose buildup for obliquely incident photon beams," Med. Phys. **14**, 393–399 (1987).
[46]T. E. Schultheiss, A. Liu, G. Olivera, J. Kapatoes, and J. Wong, "Total marrow and total lymphatic irradiation with helical tomotherapy," Med. Phys. **31**, 1845 (2004).
[47]F. R. Appelbaum *et al.*, "The use of radiolabeled anti-CD33 antibody to augment marrow irradiation prior to marrow transplantation for acute myelogenous leukemia," Transplantation **54**, 829–833 (1992).
[48]D. Hawkins, T. Barnett, W. Bensinger, T. Gooley, and J. Sanders, "Busulfan, melphalan, and thiotepa with or without total marrow irradiation with hematopoietic stem cell rescue for poor-risk Ewing-Sarcoma-Family tumors," Med. Pediatr. Oncol. **34**, 328–337 (2000).
[49]R. A. Clift, C. Dean Buckner, F. R. Appelbaum, E. Bryant, S. I. Bearman, F. B. Petersen, L. D. Fisher, C. Anasetti, P. Beatty, W. I. Bensinger, K. Doney, R. S. Hill, G. B. McDonald, P. Martin, J. Meyers, J. Sanders, J. Singer, P. Stewart, K. M. Sullivan, R. Witherspoon, R. Storb, J. A. Hansen, and E. Donnall Thomas, "Allogeneic marrow transplantation in patients with chronic myeloid leukemia in the chronic phase: A randomized trial of two irradiation regimens," Blood **77**, 1660–1665 (1991).
[50]R. Corvo, T. Lamparelli, B. Bruno, S. Barra, M. T. Van Lint, V. Vitale, and A. Bacigalupo, "Low-dose fractionated total body irradiation (TBI) adversely affects prognosis of patients with leukemia receiving an HLA-matched allogeneic bone marrow transplant from an unrelated donor (UD-BMT)," Bone Marrow Transplant **30**, 717–723 (2002).
[51]T. J. FitzGerald *et al.*, "Effect of X-irradiation dose rate on the clonagenic survival of human and experimental animal hematopoietic tumor cell lines: Evidence for heterogeneity," Int. J. Radiat. Oncol., Biol., Phys. **12**, 69–73 (1986).
[52]J. G. Rhee, C. W. Song, T. H. Kim, and S. H. Levitt, "Effect of fractionation and rate of radiation dose on human leukemic cells, HL-60," Radiat. Res. **101**, 519–527 (1985).
[53]N. Tarbell J, D. A. Amato, J. D. Down, P. Mauch, and S. Hellman, "Fractionation and dose rate effects in mice: A model for bone marrow transplantation in man," Int. J. Radiat. Oncol., Biol., Phys. **13**, 1065–1069 (1987).
[54]J. M. Cosset, G. Socie, T. Girinsky, B. Dubray, A. Fourquet, and E. Gluckman, "Radiobiological and clinical bases for total body irradiation in the leukemias and lymphomas," Semin. Radiat. Oncol. **5**, 301–315 (1995).
[55]T. Girinsky, G. Socie, H. Ammarguellat, J. M. Cosset, E. Briot, A. Bridier, and E. Gluckman, "Consequences of two different doses to the lungs during a single dose of total body irradiation: results of a randomized study on 85 patients," Int. J. Radiat. Oncol., Biol., Phys. **30**, 821–824 (1994).
[56]L. H. Gerig, J. Szanto, T. Bichay, and P. Genest, "Translating-bed technique for total-body irradiation," Phys. Med. Biol. **39**, 19–35 (1994).
[57]D. Cowen, P. Richaud, G. Marit, P. Cony-Makhoul, R. Trouette, C. Faberes, and J. Reiffers, "Regimen-related toxicity in patients undergoing BMT with total body irradiation using a sweeping beam technique," Bone Marrow Transplant **10**, 515–519 (1992).
[58]S. A. Carruthers and M. M. Wallington, "Total body irradiation and pneumonitis risk: A review of outcomes," Br. J. Cancer **90**, 2080–2084 (2004).
[59]M. Beyzadeoglu, K. Oysul, B. Dirican, F. Arpaci, A. Balkan, S. Surenkok, and Y. Pak, "Effect of dose-rate and lung dose in total body irradiation on interstitial pneumonitis after bone marrow transplantation," Tohoku J. Exp. Med. **202**, 255–263 (2004).
[60]H. J. Dobbs, A. Barrett, A. Y. Rostom, and M. J. Peckham, "Total-body irradiation in advanced non-Hodgkin″s lymphoma," Br. J. Radiol. **54**, 878–881 (1981).
[61]W. A. Tome, and J. F. Fowler, "On cold spots in tumor subvolumes," Med. Phys. **29**, 1590–1598 (2002).
[62]T. Zhang, R. Jeraj, H. Keller, W. Lu, G. H. Olivera, T. R. McNutt, T. R. Mackie, and B. Paliwal, "Treatment plan optimization incorporating respiratory motion," Med. Phys. **31**, 1576–86 (2004).